

Nanoscale

Accepted Manuscript



This is an *Accepted Manuscript*, which has been through the Royal Society of Chemistry peer review process and has been accepted for publication.

Accepted Manuscripts are published online shortly after acceptance, before technical editing, formatting and proof reading. Using this free service, authors can make their results available to the community, in citable form, before we publish the edited article. We will replace this *Accepted Manuscript* with the edited and formatted *Advance Article* as soon as it is available.

You can find more information about *Accepted Manuscripts* in the [Information for Authors](#).

Please note that technical editing may introduce minor changes to the text and/or graphics, which may alter content. The journal's standard [Terms & Conditions](#) and the [Ethical guidelines](#) still apply. In no event shall the Royal Society of Chemistry be held responsible for any errors or omissions in this *Accepted Manuscript* or any consequences arising from the use of any information it contains.

Construction of DNA Nanotubes with Controllable Diameters and Patterns by Using Hierarchical DNA Sub-tiles

Xiaolong Shi,^a Xiaoxu Wu,^a Tao Song,^{b,c,*} and Xin Li^{d,‡}

Design of DNA nanotubes is a promising and hot research branch in structural DNA nanotechnology, which is rapidly developed as a versatile method for achieving subtle nanometer scale materials and molecular diagnosing/curing devices. Multifarious methods have been proposed to achieve varied DNA nanotubes, such as using square tiles and single-stranded tiles, but it is still a challenge to develop a bottom-up assembling way of building DNA nanotubes with different diameters and patterns by using certain universal DNA nanostructure. This work addresses the challenge by achieving an approach of assembling three types of spatial DNA nanotubes with different diameters and patterns from the so-called “basic bricks”, i.e., hierarchical DNA sub-tiles. High rate of process and throughput synthesis of DNA nanotubes are observed and analyzed by atomic force microscopy. Experimental observations and data analysis suggests the stability and controllability of DNA nanotubes assembled by hierarchical DNA sub-tiles.

1 Introduction

DNA nanotechnology is the design and manufacture of artificial nucleic acid structures for nano-meter scale technological uses, such as nanometer-scale materials^{1–5}, nano-mechanical devices^{6–11}, gene disease signal diagnosis^{12–17}. Static structures have been created by researchers, for instances, two- and three-dimensional crystal lattices^{14–16,18}, nanotubes^{19–21}, polyhedral^{23–25}, and arbitrary shapes^{26–29}. Among the structures, DNA nanotubes, (also known as an especial 3D DNA nanostructure), have entailed a body of laboratory work because of the potential applications. These include containers of transporting and releasing nano-cargos, and conductive nanowires for the nanocircuits^{30,31}. Methods have been developed to establish sophisticated 3D DNA nanotubes, where DNA tiles and “single-stranded tiles (SST)” self-assembly based methods become hot in DNA nanotechnology.

In 2003, Thomas et al. initially designed a 4×4 tile consisting of four 4-arm junctions. They were oriented towards the same direction in the grid plane by controlling the distance between neighboring tile centers. Long tube-like lattices with uniform width were synthesized³². Subsequently, 3- and 6-arm DNA

tiles were designed and used to synthesize DNA nanotubes^{33,34}. Yin et al. presented a simple tile motif SST, which can be assembled into ribbons and tubes with steerable circumferences^{36,37}. Although various methods have been proposed to construct DNA nanotubes, developing a universal method still remains a challenge. Construction of DNA nanotubes with controllable diameters is becoming a promising branch in DNA nanostructure as there have been few peering results within recent years of study^{38,39}

In this work, we address the 2-fold challenge by proposing a universal approach for constructing DNA nanotubes with controllable diameters and patterns with hierarchical DNA sub-tiles. The “basic bricks” proposed here is not the 3-arm, 4-arm and 6-arm DNA tiles as designed in^{40,41}, but the sub tiles are unsymmetrical simple DNA structures, which can hierarchically assembled to 3-arm or 4-arm or 6-arm tiles and finally spatial DNA tubes with different level of programmable sticky ends. Using hierarchical DNA sub-tiles as parts, 3-, 4- and 6-arm DNA tiles can be established, from which DNA nanotubes of specific diameters and patterns can be assembled. In this way, a universal approach is achieved to construct DNA nanotubes with different diameters and patterns, where the diameters and patterns can be controlled by the structure of assembled DNA sub-tiles. DNA nanotubes assembled by 3-, 4- and 6-arm DNA tiles are visualized and analyzed by atomic force microscopy (AFM). The experimental observations suggest the stability and the controllability of DNA nanotubes, with different diameters assembled by hierarchical DNA sub-tiles. These observations indicate that the throughput and length of the DNA nanotubes assembled by 4-arm tiles are higher than the DNA nanotubes assembled by 3- and 6-arm DNA tiles. The general results

^aKey Laboratory of Image Information Processing and Intelligent Control, School of Automation, Huazhong University of Science and Technology, Wuhan 430074, Hubei, China

^bCollege of Computer and Communication Engineering, China University of Petroleum, Qingdao 266580, Shandong, China, E-mail: tsong@upc.edu.cn

^cFaculty of Engineering, Computing and Science, Swinburne University of Technology, Sarawak Malaysia, 93350, Kuching, Malaysia

^dDepartment of Gynecology 2, Renming Hospital of Wuhan University, Wuhan 430060, Hubei, China, E-mail: lixinwhu@189.cn

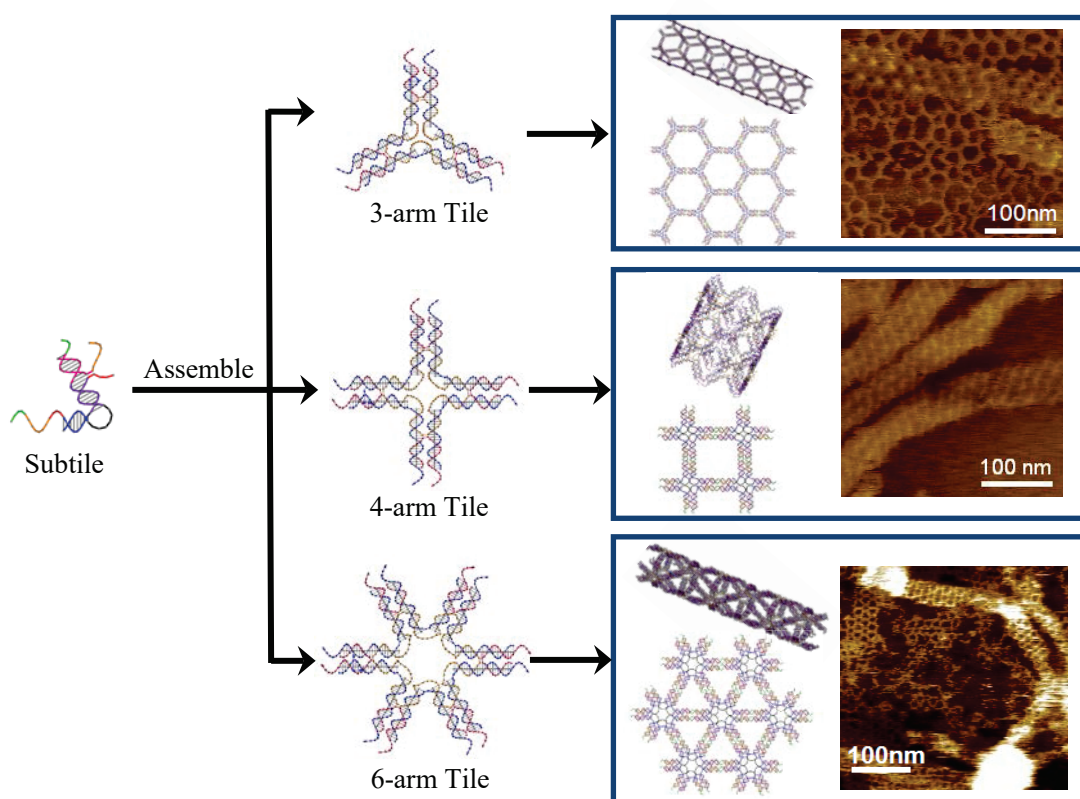


Fig. 1 The general results of using hierarchical DNA sub-tiles to assemble DNA nanotubes and lattice with controllable diameters and patterns

can be found in Figure 1.

2 Methods

2.1 Design and Modeling.

Here we elaborate the 4-arm DNA sub-tile, while the 3-arm and 6-arm DNA sub-tiles can remain being referred to as Supplementary. A 4-arm DNA tile, a cross-like DNA structure, is composed of four sub-tiles. These sub-tiles as referred to as S_1, S_2, S_3, S_4 and as illustrated in Figure 2. The sub-tiles are identical in structure but have distinct DNA domains (with different colors) in different DNA sequences.

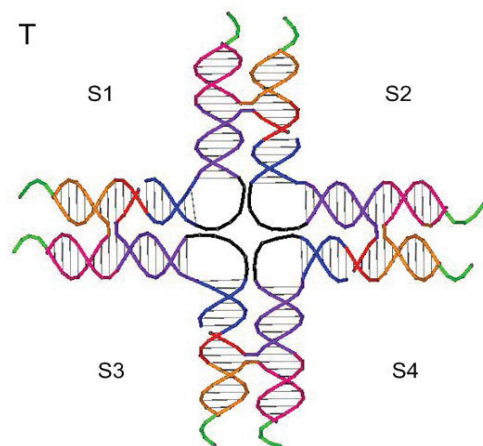


Fig. 2 A 4-arm DNA tile based on sub-tiles S_1, S_2, S_3, S_4

Each arm of the 4-arm DNA tile has two single DNA strands – sticky ends at its terminal. Magnified, each sub-tile includes three single-stranded DNA (ssDNA). For instance, sub-tile S_1 , shown in Figure 3.a, is composed of ssDNA S_{11}, S_{12} and S_{13} . DNA domains on these ssDNA are defined in a 5'-3' fashion. Domain S_{11} is constructed of 42 base pairings (bps), with five sub-domains labeled $SE_{11}, S_{11a}, S_{11b}, S_{12}$ and S_{13} . Domain S_{12} has 21 bps, grouped in three distinct sub-domains S_{21a^*}, S_{13^*} and SE_{12^*} . Domain S_{13} has 27 bps, composed by three sub-domains S_{21b^*}, S_{12^*} and $6T$ which is embedded in S_{12^*} . There are two-level sticky-ends on sub-tile strands. Sub-domains with 4-9 bps, including S_{11a} (9 bps), S_{11b} (6bps), S_{21a^*} (9 bps) and S_{21b^*} (6bps), are referred to as the first level sticky-ends, for sub-tiles to form into 4-arm DNA tiles. Sub-domains with 4 bps, including SE_{11} and SE_{12^*} , are the second level sticky-ends. Using the sticky-ends 4-arm DNA tiles can be bound, therefore assembled into 2D lattice or 3D nanotubes.

The other three sub-tiles S_2, S_3 and S_4 can be designed in a similar strategy, but with distinct domains (resp. sub-domains) and specific DNA sequences so the four sub-tiles can combine together to form 4-arm DNA tiles, see Figure 3.b.

In Figures 2 and 3, specific DNA strands are denoted by colored lines. Full lines and dotted lines of the same color indicate that they are complementary according to Watson-Crick base pairing principle and anti-parallel with each other to form double DNA strands, the imaginary and simplified DNA helices.

Sub-domains $S_{21a^*}, S_{13^*}, S_{21b^*}, S_{12^*}$ and SE_{12^*} , depicted by dotted lines are respectively complementary to domains $S_{21a}, S_{13}, S_{21b}, S_{12}$ and SE_{12} , which are depicted in full lines.

The red right angle folding line enclosed in the circle represents a bulged sub-domain of sextuple Thymine (or $6T$ loop) inserted in sub-domain S_{12^*} , in which sub-tile S_1 can be bent to specific angles thus providing the high flexibility of 4-arm DNA tiles. Bulged $6T$ sub-domains populate on all sub-tiles S_1, S_2, S_3 and S_4 . Therefore, a 4-arm tile can inflect along the two diagonal axes as-well as the horizontal and vertical axes.

Each 4-arm DNA tile can bind other four 4-arm DNA tiles by using second level sticky-ends to form lattices (see e.g. in Figure 4.a, a 4×4 lattice) and DNA nanotubes (a diagrammatic drawing of a DNA nanotube shows its spatial structure in Figure 4.b). Theoretically, lattices can continuously grow outward in all directions. DNA nanotubes are favorable in this design because each of the 4-arm DNA tiles possesses incidental curvature. The curvatures will accumulate and start the circularization of lattices as 4-arm DNA tiles oriented in the same direction connecting their counterparts. Additionally, the nanotube formation is attributed to the quick thermal annealing procedure (two hours) compared to previous experiment (over 48 hours).

It is easy to obtain 3-arm and 6-arm DNA tiles with using sub-tiles by changing the DNA sequences of the first and second sticky-ends in agreement to the 3- and 6-arm tiles. The structures of 3- and 6-arm DNA tiles are given in details in the Supplementary. Lattices and diagrammatic drawings of a DNA nanotubes assembled by 3-arm and 6-arm DNA tiles are shown in Figures 5 and 6.

The releasing holes of the DNA nanotubes shown in Figures 4, 5 and 6 are assembled by 3-, 4- and 6-arm tiles of different sizes, thus having different patterns. The obtained DNA nanotubes self-assembled by 3-, 4- and 6-arm tiles provide significantly potential applications in nano-scale. They can transport “cargos” to target circumstance in living cells and release specific chemicals, such as polymeric drugs of different sizes.

2.2 Experiment observations.

The oligonucleotides were acquired from Sangon Biotech Company with PAGE (polyacrylamide gel electrophoresis) purification. It is started by synthesizing sub-tiles S_1, S_2, S_3 and S_4 , by which 4-arm DNA tiles can be constructed. Sub-tile S_1 was constructed by one-pot annealing of ssDNA S_{11}, S_{12} and S_{13} from 94°C to room temperature in TAE buffer (10mM Mg^{2+} , 20mM Tris with pH 7.6-8.0, 2mM EDTA) over 2 hours with a final concentration of $7\mu\text{M}$ for each ssDNA. Generally, other sub-tile S_i was constructed by ssDNA S_{i1}, S_{i2} and S_{i3} with $i = 2, 3, 4$. 4-arm DNA tile was constructed by sub-tiles S_1, S_2, S_3 and S_4 to assemble DNA nanotubes. Sub-tile was respectively diluted by TAE buffer (10mM Mg^{2+} , Ph 8.0) in four epoxy resin (EP) tubes to reach a final concentration of $1\mu\text{M}$. After that, $30\mu\text{L}$ mixtures of the four sub-tiles with the same concentration were annealed from 45°C to room temperature in a Styrofoam box for over 20 hours. After annealing, the sample was kept in a refrigerator at 4°C before being examined by AFM.

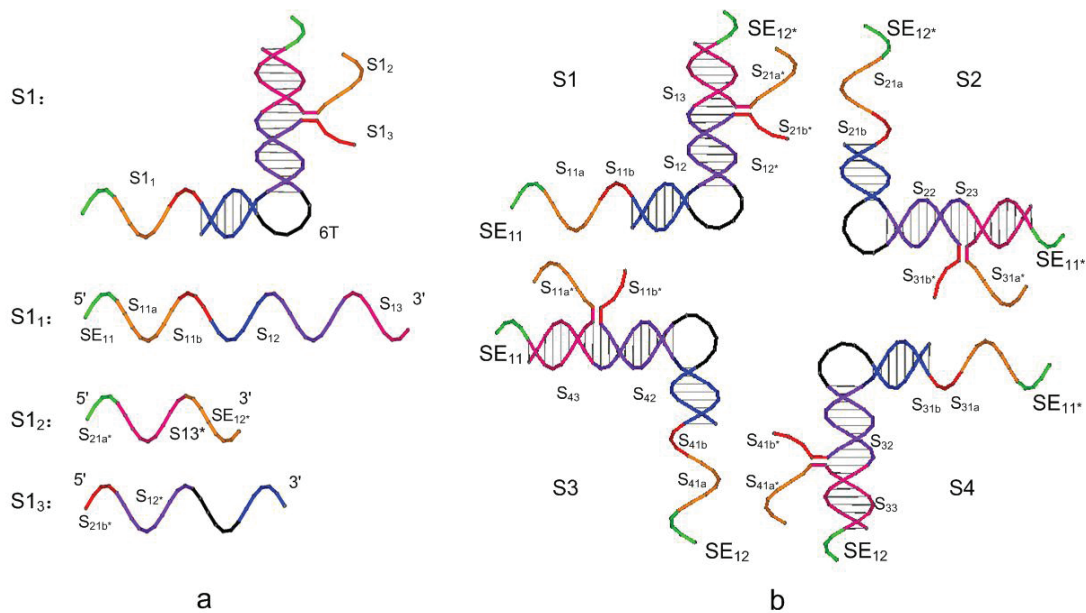


Fig. 3 a. Sub-tile S_1 and DNA subdomains on ssDNA S_{11} , S_{12} and S_{13} ; b. sub-domains and specific DNA sequences on sub-tiles S_2 , S_3 and S_4 .

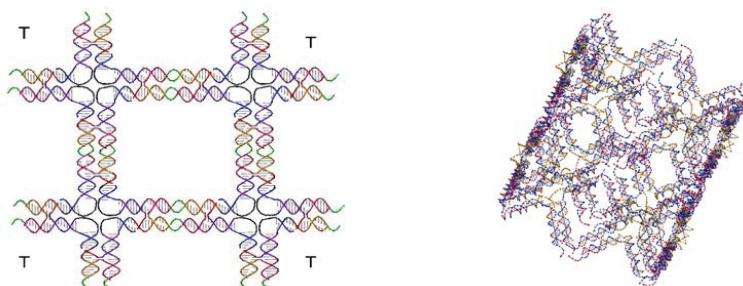


Fig. 4 a. 4-arm DNA tiles self-assemble together into a 4×4 lattice; b. a DNA nanotube assembled by 4-arm DNA tiles.

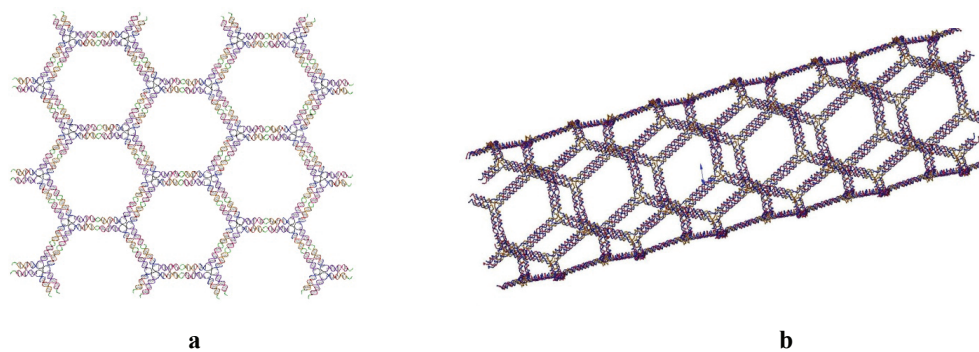


Fig. 5 Lattices and a diagrammatic drawing of a DNA nanotubes assembled by 3-arm DNA tiles.

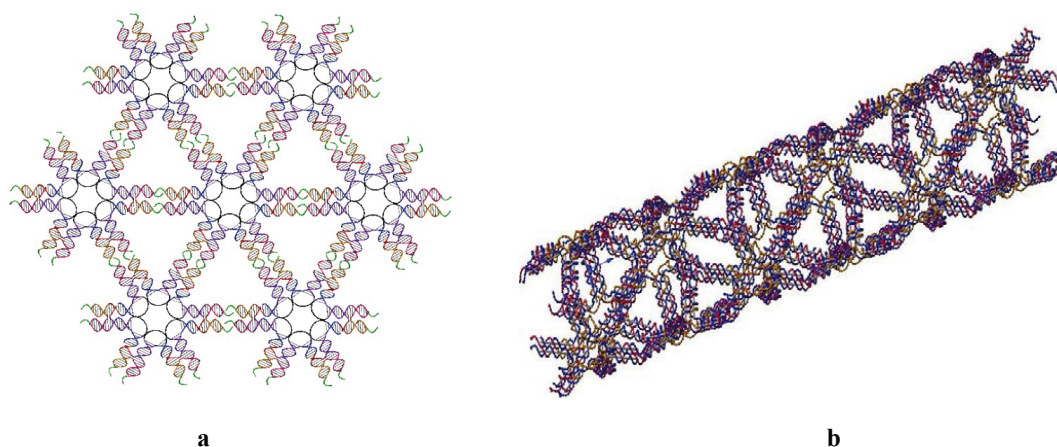


Fig. 6 Lattices and a diagrammatic drawing of a DNA nanotube assembled by 6-arm DNA tiles.

The nanotubes hierarchically assembled from the same sub-tile structure are observed by AFM as follows. $5\ \mu\text{L}$ samples of 3-arm, 4-arm or 6-arm nanotubes are dropped onto a fresh cleaved mica surface. The sample is kept at room temperature for 3 minutes for absorption, and then then $30\ \mu\text{L}$ TAE buffer are added to the mica and the tip on fluid cell, respectively. AFM images are obtained by using a Bruker Multimode-8 Nanoscope (Billerica, MA, USA) under ScanAsyst mode with a ScanAsyst Fluid+ tip. The engaged force of the ScanAsyst mod is maintained under 0.02V to ensure gentle touch on the DNA nanotube, and the scan rate was kept under $1\ \text{HZ}$ during scanning to get the details.

The AFM image, Leftward in Figure 7, shows that the long nanotubes ($1\ \mu\text{m}$ - $5\ \mu\text{m}$) were successfully constructed as expected. The AFM image, Rightward in Figure 7, shows the mean diameter of the DNA nanotubes is about 53.25nm . This AFM image was taken under ScanAsyst mod of Multimode-8, and engaged force was kept under $0.02\ \text{V}$ with scan rate being $1\ \text{HZ}$.

The four nanotubes were selected randomly to calculate the mean diameter of the nanotubes with the formula:

$$(d_1 + d_2 + d_3 + d_4)/4 = 213\text{nm}/4 = 53.25\text{nm}.$$

The diameter of nanotubes formed by 4-arm tiles is in the range of 40.6nm to 61.6nm , which could be flattened due to the strength of the interaction between DNA, Mg^{++} , and the mica or squashed by the force of AFM tips during scanning. What we can see in Figure 8(a) is that there is a single lattice layer unpacked at the end of the nanotube. The appearance of the unpacked lattice layer suggests that the nanotube was broken and flattened into lattice while interacting with the mica, through the charge shielding Mg^{2+} in the buffer. By the measurement of the unpacked single lattice layer in Figure 8, we averaged the distance between the two neighboring 4-arm DNA tiles at 17.22nm and the edge of a tetragon at 13.5nm . These values are in reasonable agreement with our design ($17.6\ \text{nm}$ and $13.6\ \text{nm}$, respectively).

This AFM image is taken under ScanAsyst mod of Multimode-8 with engaged force being kept under 0.02V . The scan rate is $1\ \text{HZ}$.

The 3-arm and 6-arm DNA tiles were also constructed to synthesize DNA nanotubes, (please refer to the supplementary infor-

mation at Section 2). AFM images of DNA nanotubes assembled by 3-arm and 6-arm DNA tiles are shown in Figures 9 and 10, which is taken under ScanAsyst mod of Multimode-8 with engaged force being kept under 0.02V and scan rate being $1\ \text{HZ}$.

Hexagonal and triangular crystal lattices were constructed by the 3-arm and 6-arm DNA tiles that can be clearly exhibited. The rigidities of the mesh in the hexagonal and triangular crystal lattices are much higher than that of the tetragonal meshes rendering them less bendable and capable of to forming into nanotubes. The productivity of the nanotubes is much lower than that of the 4-arm DNA tile nanotubes.

The AFM image shown in Figures 9 and 10 are taken under ScanAsyst mod of Multimode-8, where the engaged forces are kept under 0.02V and scan rates are $0.5\ \text{HZ}$, respectively.

The nanotubes are with different diameters even if same design scheme and samples. With our experiment of sub tiles, it is found that the diameter of nanotubes varied with the following two factors.

- The first one is the sticky ends of sub tiles we logically designed with which 3-, 4- and 6-arm DNA tiles and spatial tubes are expected. The diameter of spatial tubes varied with the number of arms of tiles consisted of sub tiles. It is assumed that the sub tiles assembled to 3-, 4- or 6-arm DNA tiles as we designed, and 2 or more DNA tiles assembled to one layer nanoribbon first. The more arms a DNA tile has, the more strength the ribbon that formed has to curve and finally curling to a closed tube. That's the reason why the 3-arm tile formed 140nm tube and 4-arm tile formed 50nm tube and 6-arm tile formed 20nm tube, although these tubes are hierarchically assembled from the same sub tile structure.
- The second one is the store time of samples after annealing. With long time stored in $4\ \text{degree}$ refrigerator for 1 month or more, the tubes could merged to a bigger one, and this might due to the fact that nanotubes formed through annealing have just clasped to a local minimum of free energy. With long time storage, the tube slowly releases the internal tension of bend double helixes of DNA and form a bigger

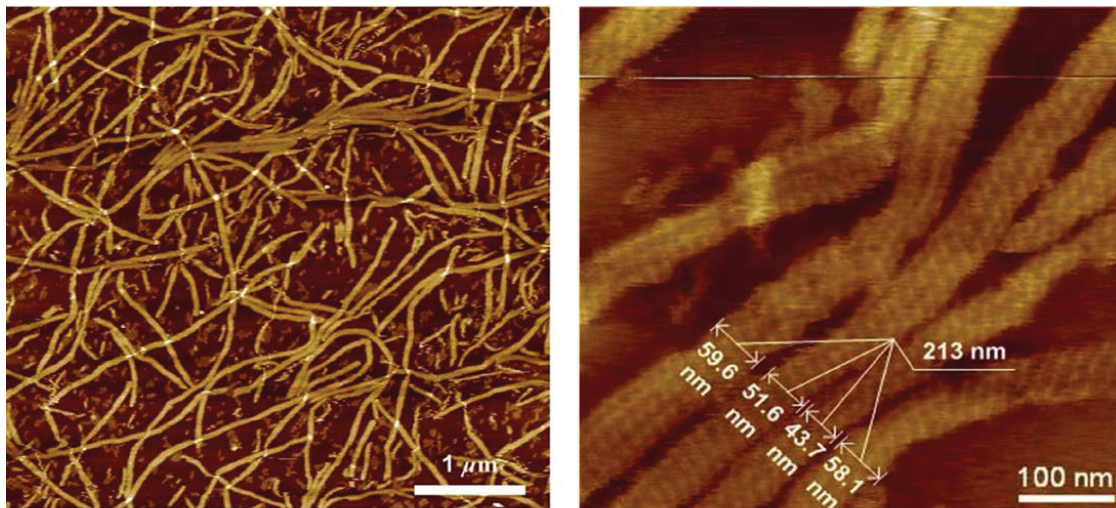


Fig. 7 **Leftward**, AFM images of DNA nanotubes assembled from 4-arm DNA tiles. AFM image of 4-arm DNA tile nanotubes with $5\mu\text{m}\times 5\mu\text{m}$ scan size; the data height range is 0-15nm. Nanotubes measuring at 5 μm or longer were observed. **Rightward**, AFM image of nanotubes in detail with $800\text{nm}\times 800\text{nm}$ scan size; the data height range is 0-15nm.

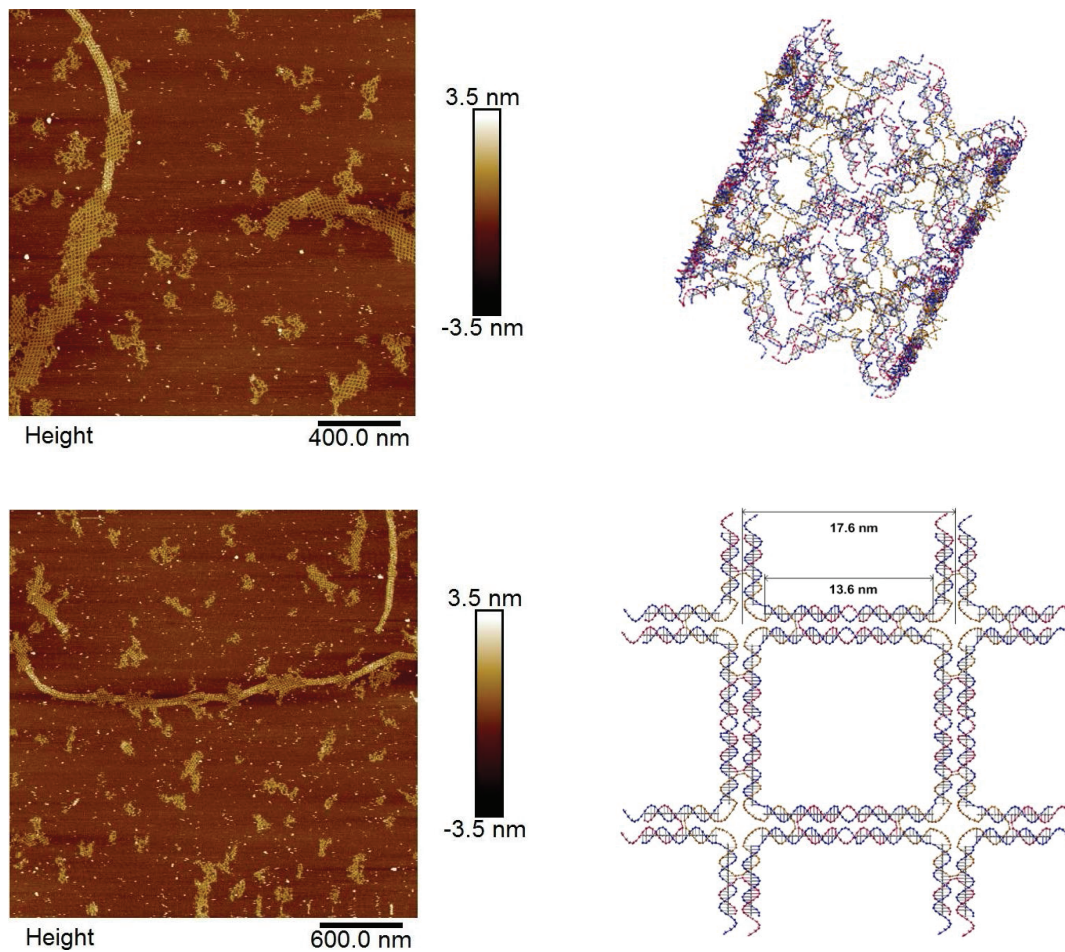


Fig. 8 AFM images of the local-patterns unfold by the nanotube. (a) AFM image of a single lattice layer unpacked at the end of the nanotube (left) with 400 nm scan bar and height range of 7nm; and its simulation graph (right). (b) The distance between the two neighboring 4-arm DNA tiles is 17.22 nm versus 17.6 nm for the designed model, and the length of 4-arm nanotube is more than $3\mu\text{m}$.

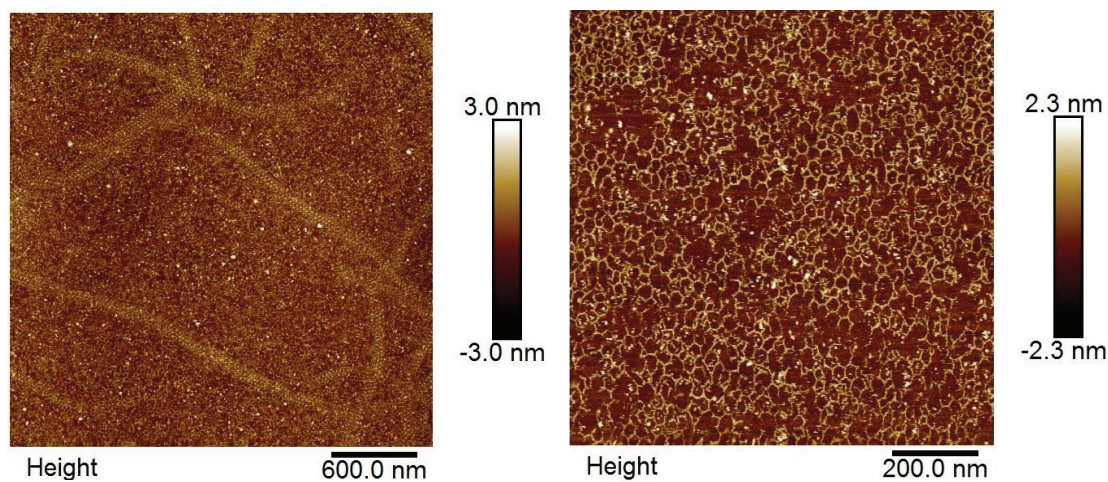


Fig. 9 AFM images of DNA nanotubes constructed by 3-arm DNA tiles. **Leftward**, AFM image of 3-arm DNA tile nanotubes with $3\mu\text{m}\times 3\mu\text{m}$ scan size; the data height range is -3-3nm. More than 6 nanotubes with uniform diameters 140 nm were observed. **Rightward**, AFM image of opened 3-arm nanotubes with $1\mu\text{m}\times 1\mu\text{m}$ scan size in detail; the data height range is -2.3-2.3nm, and the hexagonal crystal lattice assembled by sub-tiles can be clearly observed.

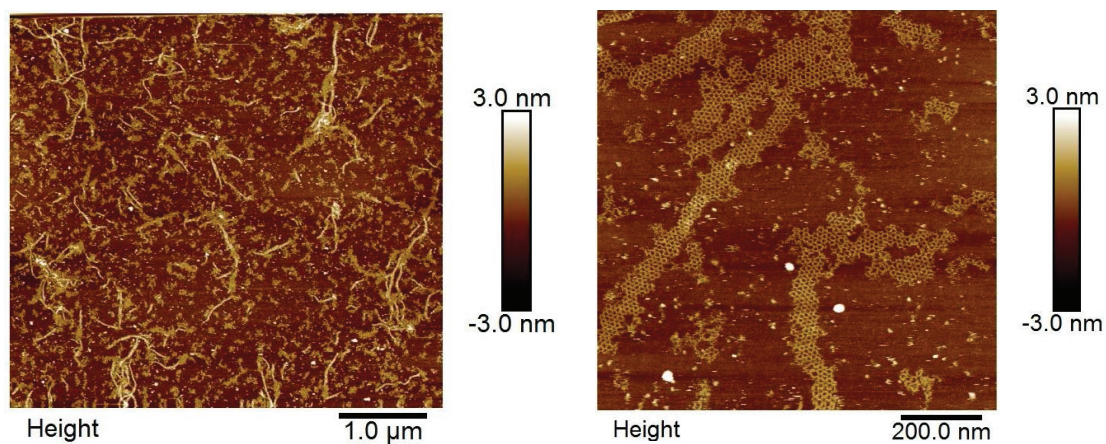


Fig. 10 AFM images of DNA nanotubes constructed by 6-arm DNA tiles. **Leftward**, AFM image of 6-arm DNA tile nanotubes with $5\mu\text{m}\times 5\mu\text{m}$ scan size; the data height range is -3-3nm. DNA Nanotubes were formed as designed with a mass of unpacked lattice layer, and the dimension of the DNA nanotube is about 20nm. **Rightward**, AFM image of 6-arm DNA tile DNA nanotubes with $1\mu\text{m}\times 1\mu\text{m}$ scan size; the data height range is -3-3nm.

tube. That might be the reason why we could find difference of diameters of nanotubes even if same design scheme and samples.

3 Conclusions

In this paper, three kinds of DNA nanotubes were constructed by 3-, 4-, and 6-arm DNA tiles using the two leveled sticky-ends sub-tile strategy as previously mentioned. The 4-arm tile shown in Fig. 2 and nanotubes shown in Fig. 7 are very much resemble the un-corrugated nanotubes previously described in Fig. 1 in Ref[2]. It needs to clarify that our strategy with using sub-tiles can also construct 2-arm, 3-arm, and even 6-arm tiles and nanotubes from sub-tiles with different diameters and patterns. The large populations of long ribbon-like nanotubes were examined under AFM scope. The AFM images of DNA nanotubes based on 3-, 4- and 6-arm DNA tiles clearly suggest that the throughput of DNA nanotubes based on the 4-arm DNA tiles is higher than that of the nanotubes constructed by 3-arm and 6-arm DNA tiles. Since the widths of observed nanotube could not be predicted beforehand, we just observe the nano-tubes by AFM and record the diameters of the nano-tubes assembled by different DNA tiles. The high productivity of DNA nanotubes based on 4-arm DNA tiles could be expected and can be explained by the stability of this kind of nanotubes structure. The resulting productivity and structure still remain dependent on the geometry of the 4-arm DNA tiles and the tetragonal meshes on the nanotubes.

The rigidity of tetragonal meshes is lower than that of hexagonal meshes shaped by 3-arm DNA tiles, and triangular meshes enclosed by 6-arm DNA tiles. Therefore, 4-arm DNA tiles are more prone to assemble into nanotubes than 3-arm and 6-arm DNA tiles. The intrinsic angles of 3-, 4- and 6-arm DNA tiles are important to the formation of DNA tiles with 3-5Ts in each turning corners of 3-, 4- or 6-arm tiles in^{2,40,41}. The proposed novel sub tile here work as “basic brick” to assemble 3-, 4- and 6-arm DNA tiles. By adding 6-Ts to the turning corn of sub tile demonstrated in Fig. 3.b, we give enough flexibility to the sub tile to assemble to 3-, 4- and 6-arm DNA tiles and spatial tubes with programmable sticky ends.

Nowadays, people prefer to use smaller weight (nts) of DNA building blocks in order to enhance final production yield. But 3-, 4- and 6-arm DNA tiles are relatively heavier. Smaller weight of DNA building blocks will leading to high yield. That's the reason why sub tile strategy is developed. The sub tile consists of 3 single stranded DNA, which is much lighter than the heavy DNA tile structure. With the sub tile strategy, we get pretty high production yield such that it is not necessary to use gel purification in each step. With carefully ratio control, all the samples could be directly put under AFM for observation after anneal.

In the field of medicine delivery, the resulting DNA nanotubes can be applied to drug delivery by tethering chemical components on the nanotubes's walls or encapsulating drug cargos in the tubes³⁸. As for nanocircuitries, DNA nanotubes can also be used as conductive nanowires by binding metallic nanoparticles to engineer sophisticated nanocircuits³³. For morphology aspects, exerting mixed 3-, 4-, 6-arm and other multi-arm DNA tiles to form multi-shaped meshes, for example, hexagonal, tetragonal

and triangular and other polygonal mesh mixtures, may lead to nanotubes in high dimensions.

Acknowledgement

This work is supported by the National Science Foundation of China (Grant Nos. 61272071, 61272022, 61402187, 61370105, 61572213 and 61502535) and Science Foundations of Hubei Province (No. 2014CFB730), China Postdoctoral Science Foundation funded project (2016M592267), and Fundamental Research Funds for the Central Universities (R1607005A).

References

- 1 C. A. Mirkin, R. L. Letsinger, R. C. Mucic and J. J. Storhoff, *Nature*, 1996, **382**, 607
- 2 H. Yan, S. H. Park, G. Finkelstein, J. H. Reif and T. H. Labean, *Science*, 2003, **301**, 1882–1884
- 3 N. C. Seeman, *Nature*, 2003, **421**, 427
- 4 R. J. Macfarlane, B. Lee, M. Jones, N. Harris, G. C. Schatz and C. A. Mirkin, *Science*, 2011, **334**, 204–208
- 5 Y. Geng, E. Pound, S. Gyawali, J. R. Ashton, J. Hickey, A. T. Woolley, J. N. Harb and J. Liu, *ACS Nano*, 2011
- 6 H. Yan, X. Zhang, Z. Shen and N. C. Seeman, *Nature*, 2002, **415**, 62
- 7 R. P. Goodman, M. Heilemann, S. Doose, C. M. Erben and A. N. Kapanidis, *Nature Nanotechnology*, 2008, **3**, 93
- 8 Y. Tian, Y. He, Y. Chen, P. Yin and C. Mao, *Angewandte Chemie*, 2005, **44**, 4355–4358
- 9 K. Lund, A. J. Manzo, N. Dabby, N. Michelotti, A. Johnsonbuck, J. Nangreave and H. Yan, *Nature*, 2010, **465**, 206
- 10 X. Shi, Z. Wang, C. Deng, T. Song, L. Pan and Z. Chen, *PLOS ONE*, 2014, **9**, e108856–e108856
- 11 Y. He and D. R. Liu, *Nature Nanotechnology*, 2010, **5**, 778
- 12 P. Rodgers and J. Heath, 2010, *Nature Publishing Group*
- 13 H. Lee, A. K. R. Lyttonjean, Y. Chen and K. T. L. et. al., *Nature Nanotechnology*, 2012, **7**, 389
- 14 E. Winfree, F. Liu, L. A. Wenzler and N. C. Seeman, *Nature*, 1998, **394**, 539
- 15 H. Yan, T. H. Labean, L. Feng and J. H. Reif, *Proceedings of the National Academy of Sciences*, 2003, **100**, 8103–8108
- 16 S. H. Park, C. Pistol, S. J. Ahn, J. H. Reif, A. R. Lebeck, C. Dwyer and T. H. Labean, *Angewandte Chemie*, 2006, **118**, 749–753
- 17 H. D. Hill, R. J. Macfarlane, A. J. Senesi, B. Lee, S. Y. Park and C. A. Mirkin, 2008
- 18 J. Zheng, J. J. Birktoft, Y. Chen, T. Wang, R. Sha, P. E. Constantinou, S. L. Ginell, C. Mao and N. C. Seeman, *Nature*, 2009, **461**, 74
- 19 K. Williams, P. T. M. Veenhuizen, B. G. D. L. Torre, R. Eritja and C. Dekker, *Nature*, 2002, **420**, 761
- 20 H. Maune, S. Han, R. D. Barish, M. Bockrath, W. A. Goddard, P. W. K. Rothemund and E. Winfree, *Nature Nanotechnology*, 2010, **5**, 61
- 21 D. Liu, S. H. Park, J. H. Reif and T. H. Labean, *Proceedings of the National Academy of Sciences*, 2004, **101**, 717–722

- 22 bellot2013dna G. Bellot, M. A. McClintock, J. J. Chou and W. M. Shih, *Nature Protocols*, 2013, **8**, 755–770
- 23 Y. He, T. Ye, M. Su, C. Zhang, A. E. Ribbe, W. Jiang and C. Mao, *Nature*, 2008, **452**, 198
- 24 N. C. Seeman, *Nano Letters*, 2010, **10**, 1971–1978
- 25 C. Zhang, S. H. Ko, M. Su, Y. Leng, A. E. Ribbe, W. Z. Jiang and C. Mao, 2009
- 26 E. S. Andersen, M. Dong, M. Nielsen and J. Kjems, *Nature*, 2009, **459**, 73–76
- 27 N. C. Seeman, Z. Shen, H. Yan and T. Wang, *Journal of the American Chemical Society*, 2004, **126**, 1666–1674
- 28 S. J. Tan, M. J. Campolongo, D. Luo and W. Cheng, *Nature Nanotechnology*, 2011, **6**, 268
- 29 H. Yan, Y. Liu, J. Nangreave and F. Zhang, 2014
- 30 H. Yan, J. Nangreave, G. Zou, C. Chen and D. Qiu, *Journal of the American Chemical Society*, 2012
- 31 T. Yoshie, A. Scherer, J. Hendrickson, G. Khitrova, H. M. Gibbs, G. Rupper, C. Ell, O. B. Shchekin and D. G. Deppe, *Nature*, 2004, **432**, 200
- 32 T. H. Labean and S. H. Park, *Nanotechnologies for the Life Science*, 2007, Wiley Online Library
- 33 S. G. Wang, R. Wang, P. J. Sellin and Q. Zhang, *Biochemical and Biophysical Research Communications*, 2004, **325**, 1433–1437
- 34 M. Endo, K. Hidaka, T. Kato, K. Namba and H. Sugiyama, *Journal of the American Chemical Society*, 2009
- 35 yin2008programming P. Yin, R. F. Hariadi, S. Sahu, H. M. T. Choi, S. H. Park, T. H. Labean and J. H. Reif, *Science*, 2008, **321**, 824–826
- 36 S. H. Park, P. Yin, Y. Liu, J. H. Reif, T. H. Labean and H. Yan, 2004
- 37 H. Dietz, S. M. Douglas and W. M. Shih, *Science*, 2009, **325**, 725–730
- 38 O. I. Wilner, R. Orbach, A. Henning, C. Teller, O. Yehezkeili, M. Mertig, D. Harries and I. Willner, 2011
- 39 X. Shi, W. Lu, Z. Wang, L. Pan, G. Cui, J. Xu and T. H. Labean, *Nanotechnology*, 2014, **25**, 75602
- 40 Y. He, Y. Chen, H. Liu, A. E. Ribbe and C. Mao, *Journal of the American Chemical Society*, 2005, **127**, 12202.
- 41 Y. He, Y. Tian, A. E. Ribbe and C. Mao, *Journal of the American Chemical Society*, 2006, **128**, 15978.